Title: Pyrolysis Kinetics of Poly(L-lactide) with Carboxyl and Calcium Salt End Structures

Authors: Yujiang Fan[a,b], Haruo Nishida[a,*], Shinya Hoshihara[a], Yoshihito Shirai[b], Yutaka Tokiwa[c], and Takeshi Endo[a,d]

[a] Molecular Engineering Institute, Kinki University, 11-6 Kayanomori, Iizuka, Fukuoka 820-8555, Japan

[b] Graduate School of Life Science and System Engineering, Kyushu Institute of Technology, 1-1 Hibikino, Kitakyushu, Fukuoka 808-0196, Japan

[c] National Institute of Advanced Industrial Science and Technology (AIST), AIST Tsukuba Central 6, Tsukuba, Ibaraki 305-8566, Japan

[d] Faculty of Engineering, Yamagata University, 4-3-16 Jonan, Yonezawa, Yamagata 992-8510, Japan

[*]Corresponding author.

Tel / Fax: +81-948-22-5706.

E-mail address: hnishida@mol-eng.fuk.kindai.ac.jp (H. Nishida)

Abstract

To clarify the pyrolysis mechanism of poly(L-lactide), which has been reported as complex, the thermal decomposition of carboxyl type and calcium ion end capped PLLA (PLLA-H and PLLA-Ca, respectively) was investigated by means of thermogravimetric analysis (TG), and pyrolysis-gas chromatography-mass spectrometry (Py-GC-MS). The TG data revealed that PLLA-Ca has a lower pyrolysis temperature (220~360°C) than that of carboxyl type PLLA-H (280~370°C). The apparent activation energy of the decomposition reaction was estimated from TG curves at different heating rates by plural methods to be 176 and 98 kJ mol^{-1} for PLLA-H and PLLA-Ca, respectively. Further kinetic studies indicated that PLLA-H degraded mainly through a random reaction with a pre-exponential factor $A=2.0\times10^{12}$ s^{-1}, whereas PLLA-Ca degraded by way of a 1^{st}-order reaction with $A=8.4\times10^{5}$ s^{-1}. Pyrolysis products of PLLA-H were composed of lactides and other cyclic oligomers, while the degradation products of PLLA-Ca were principally lactides. The main reaction pathway for PLLA-H pyrolysis was regarded as the random transesterification, whereas for PLLA-Ca pyrolysis the unzipping depolymerization process was dominant.

Keywords

Kinetics, pyrolysis, thermal degradation, poly(L-lactide), poly(L-lactic acid), depolymerization, random degradation, simulation, thermogravimetric analysis.

1. Introduction

Poly(L-lactic acid), or poly(L-lactide)(PLLA) belongs to a group of biodegradable polymers. It has received much interest for its medical, pharmaceutical, and environmental applications [1-3]. The basic raw material of PLLA is L-lactic acid, which is produced by the fermentation of carbohydrates from renewable sources, such as corn, potato and other agriculture products, making PLLA an alternative to conventional petroleum based plastics. PLLA has many good properties such as mechanical strength, transparency, and compostability [4-6]. Thus, recently, PLLA and related copolymers have attracted industrial attention for use as commodity resins [7]. Commonly, PLLA is prepared by the ring-opening polymerization of L-lactide, a cyclic dimmer of L-lactic acid [8-10]. This reaction is an equilibrium reaction in which the concentration of residual L-lactide depends on temperature [11]. Therefore, the L-lactide is regenerated through the thermal degradation process of PLLA, making PLLA a promising candidate for feedstock recycling plastics.

However, the thermal degradation of PLLA is more complex than the simple reaction that gives lactide. Significant amounts of other volatile decomposition products are also created during the pyrolysis [5,12,13]. In order to control the decomposition in favor of the desired product, the thermal degradation mechanisms of PLLA need to be carefully analyzed. Studies on PLLA pyrolysis have been reported by several groups [12-21]. McNeill and Leiper investigated the degradation of PLLA under both controlled heating conditions and isothermal conditions [12,14]. They reported that the main products were cyclic oligomers, including lactide. Other lower boiling point products, such as carbon dioxide, acetaldehyde, ketene, and carbon monoxide were also produced. In their research they employed a 1^{st}-order reaction kinetic equation to calculate the apparent activation energy, *Ea*, as 119 kJ mol^{-1} in the range of 240-270°C. Kopinke and co-workers reported a multi step process for PLLA pyrolysis. They found that intra-molecular transesterification was a dominant degradation pathway, and that pyrolysis behavior was different between pure and Sn-containing PLLAs [13,15]. Cam et

al. also reported that compounds of metals, such as Sn, Zn, Al and Fe, had a great influence on the pyrolysis behavior of PLLA [16]. In 1999, Babanalbandi et al. [17] reported *Ea* values for PLLA using isothermal methods. Their results showed that at first the *Ea* value decreased from 103 to 72 kJ mol^{-1} with increase in weight loss and then increased up to a value of 97 kJ mol^{-1}. They postulated that the PLLA degradation process follows more complex kinetics, even at low conversion. Then, very recently, Aoyagi et al. studied the degradation behavior of PLLA [21]. In their research, they found that the *Ea* values changed in the range 80-160 kJ mol^{-1} with the change in weight loss. They concluded that the pyrolysis of PLLA involved more than two mechanisms.

To clarify each elementary reaction of the complex pyrolysis mechanism and the kinetics of PLLA, we studied the pyrolysis behavior of the rigorously purified carboxyl end PLLA (PLLA-H), which has very low metal content, and PLLA containing different kinds of metals in its end structure. In this paper, the pyrolysis behavior of PLLA-H and calcium ion end capped PLLA (PLLA-Ca) are reported. This study is mainly focused on thermogravimetric analysis (TG). The volatile products were also studied using several techniques, including NMR, GC, and Py-GC-MS spectrometry. Kinetic parameters were evaluated by simulated analyses of TG curves, and the effect of the end structures on the kinetics were discussed.

2. Experimental

2.1. Materials

Monomer, L-lactide, was obtained from Shimadzu Co. Ltd. It was composed of 99.4% L-lactide and 0.6% *meso*-lactide according to a gas chromatography (GC) measurement. This monomer was recrystallized from dry toluene, repeated three times, followed by recrystallization from dry ethyl acetate. After the purification, *meso*-lactide was not detectable by GC. The vacuum dried L-lactide was stored in a N_2 atmosphere. Catalyst, Sn

2-ethylhexanoate, obtained from Wako Pure Chemical Industries, Ltd., was distilled under reduced pressure before use. Calcium hydride was purchased from Kanto Chemical Co., Inc. and used as received. The ammonia solution (25%) and hydrochloric acid (1 **M**) produced by Wako Pure Chemical Industries, Ltd., specifically for their atomic absorption spectrophotometry applications were used as received.

2.2. Preparation of poly (L-lactide)

Poly(L-lactide) was synthesized by ring-opening polymerization catalyzed by Sn 2-ethylhexanoate, {[$Sn(Oct)_2$)). An initiator/monomer molar ratio of 1/4000 in feed and a multi-temperature process (150°C/0.5h+130°C/5h+110°C/13h+90°C/12h) were employed in the polymerization. For eliminating the Sn catalyst and low molecular weight residues from the product, purification was conducted in three stages; first extracting the catalyst and residues from the PLLA/chloroform solution with 1M HCl aqueous solution, then washing with distilled water until the aqueous phase became totally neutral, and finally precipitating the polymer in methanol. The purified polymer, PLLA-H, was dried for 24 h at room temperature *in vacuo*.

The calcium ion end capped sample (PLLA-Ca) was prepared by treating the polymer/THF solution (2g in 200 mL) with CaH_2 (0.2g, 4.76mmol) at room temperature for 1 h. After filtrating off the unreacted CaH_2, the PLLA-Ca was precipitated in methanol, and dried *in vacuo*.

For preparing PLLA-H and PLLA-Ca films, each chloroform solution of the corresponding polymer was cast in a glass Petri dish. After evaporation of the solvent, the formed film was washed by methanol and then vacuum dried.

2.3. Dynamic pyrolysis

Thermogravimetric analysis (TG) was conducted on a Seiko Instrumental Inc. EXSTAR 6200 TG/DTA system in an aluminium pan under a constant nitrogen flow (100 mL min^{-1}) using about 5 mg of the PLLA film sample. For each sample, prescribed heating rates of 1, 3, 5, 7, and 9 K min^{-1} were applied from room temperature to 400°C. The pyrolysis data were collected at regular intervals (about 20 times K^{-1}) by an EXSTAR 6000 data platform, and recorded into an analytical computer system.

2.4. Pyrolysis of poly (L-lactide) in glass tube oven

About 200 mg of the PLLA sample was put into a Shibata GTO-350D glass tube oven. The oven was then filled with nitrogen, heated gradually to 350°C and then kept at this temperature for 20min. The distilled components were collected and analyzed by infrared spectroscopy (IR), nuclear magnetic resonance (NMR) spectroscopy and gas chromatography (GC).

2.5. Measurements

GC measurements were recorded on a Shimadzu GC-9A gas chromatograph with a Varian cyclodextrine-β-236M-19 capillary column (0.25mm$\times$50m) using helium as the carrier gas. The column and injector were set isothermally at 150 and 220ºC, respectively. The sample (3mg) was dissolved in acetone (1mL) and 1μL of the solution was injected. The peaks for meso-, L,L-, and D,D-lactide were identified by comparison with pure substance peaks. Gel permeation chromatograph (GPC) was measured on a Tosoh HLC-8220 GPC system at 40ºC using Tosoh TSKgel Super HM-H column and chloroform eluent (0.6mL min^{-1}). Low polydispersity polystyrene standards with *Mn* from 560 to 113,200 were used for calibration.

The residual metal content in the PLLA samples was measured with a Shimadzu ICPS-8000 interactively coupled plasma spectrometer (ICP) and a Shimadzu AA-6500F atomic absorption flame emission spectrophotometer (AA). The samples were degraded by 25% ammonia solution, dissolved in 1**M**-hydrochloric acid, and then measured by ICP and AA.

^{1}H-NMR spectra were recorded on a Varian INOVA400 NMR spectrometer operating at 400 MHz for proton investigation in chloroform-*d* solution using tetramethylsilane as the internal standard. Infrared (IR) spectra were recorded from KBr pellets on a Nicolet Avatar 360 FT-IR spectrometer.

Pyrolysis-gas chromatograph/mass spectra (Py-GC-MS) were measured on a Frontier Lab double-shot pyrolyzer PY-2020D with a Frontier Lab SS-1010E selective sampler and a Shimadzu GCMS-QP5050 chromatograph/mass spectrometer. High purity helium at 50mL/min was used as carrier gas. The volatile products were analyzed with an Ultra Alloy^{+}-5 capillary column (30m x 0.25mm i.d.; film thickness, 0.25μm). A PLLA sample was put in the pyrolyzer and heated from 100 to 400ºC at a heating rate of 10ºC min^{-1}. The volatile pyrolysis products were conducted into the GC through the selective sampler. The temperature of column oven was set at 40°C at first. After the pyrolysis process had finished, the column was heated according to the following program: 40ºCfor 1 min; 40-120ºC at 5ºC min^{-1}; 120-320ºC at 20ºC min^{-1}; 320°C for 13 min. Mass spectrum measurements were recorded 2 times s^{-1} during this period.

3. Results and discussion

3.1. Preparation of PLLA-H and PLLA-Ca

PLLA was synthesized through the ring-opening polymerization catalyzed by Sn 2-ethylhexanoate {Sn(Oct)$_2$}. The multi-temperature process allowed the polymerization to start promptly and quickly proceed to the solid phase. After the polymerization, Sn

compounds in the PLLA were eliminated by liquid-liquid extraction using 1**M** HCl aqueous solution. Number average molecular weight (*Mn*) and polydispersity (*PDI*) of the obtained purified PLLA (PLLA-H) were 138000 and 1.83, respectively. Using ICP analysis the PLLA-H was found to contain 9 ppm of Sn, which was of the order of the lower limit of detection under these experimental conditions. Considering the Mark-Houwink-Sakurada constants for PLLA [22-24], the Sn content indicated that at least about 99% of the chain ends were free of Sn.

It has been reported that a trace amount of residual water is the actual initiator in the $Sn(Oct)_2$ catalyzed polymerization, leading to the carboxylic acid chain end [24]. Another end structure is generally assumed to be Sn alkoxide as polymerized, which would finally change to alcohol during the purification process [25]. Because of its high molecular weight, the end structure of the PLLA-H cannot be directly confirmed. Thus, low molecular weight L-lactic acid oligomer (OligoLLA, *Mn* = 1130) was synthesized and purified through a similar procedure to that described above, then measured by means of ^{1}H-NMR and IR. In the ^{1}H-NMR spectrum of the OligoLLA-H, weak quartet and doublet peaks at 4.28 and 1.49 ppm, assigned to -C***H***(CH_3)-OH and -CH(C***H*****$_3$**)-OH, were clearly observed in addition to the main quartet and doublet peaks at 5.16 and 1.59 ppm for -C***H***(CH_3)-OCO- and -CH(C***H*****$_3$**)-OCO- in the main chain, respectively [25]. No other peaks for methyne and methylene protons were detected. IR spectrum of the OligoLLA-H also showed an absorption peak at about 3400cm^{-1} for the hydroxyl group. From these results, it is reasonably inferred that the end structures of purified PLLA (PLLA-H) are mostly the carboxylic acid and hydroxyl group.

To prepare the calcium ion end capped PLLA (PLLA-Ca), the PLLA-H was treated with calcium hydride (CaH_2) and followed by precipitation into excess methanol. This treatment caused a decrease in the molecular weight (*Mn*=94,200) and an increase in the *PDI* (1.95). The obtained PLLA-Ca had 121 ppm of calcium content. To confirm changes in the end structures, the OligoLLA-H was also treated by CaH_2 in the same manner and analyzed by

AA, ^{1}H-NMR, and IR. The OligoLLA treated by CaH_2 (OligoLLA-Ca) had 4014 ppm of calcium content. IR spectrum of the OligoLLA-Ca showed a new absorption peak at 1650cm^{-1} for the carbonyl group of salt form, indicating the formation of calcium salt at the carboxylic acid end. On the other hand, the change in the hydroxyl group end was determined by a reaction of butyl lactate with CaH_2 in THF as model reaction. The ^{1}H-NMR spectrum of the CaH_2-treated butyl lactate indicated no change in the hydroxyl proton under the reaction conditions. Considering that the polymer has many fewer hydroxyl groups, the hydroxyl group end of PLLA-Ca would be kept in the hydroxyl group form. From these results, considering the Mark-Houwink-Sakurada constants for PLLA, the calcium content (121 ppm) of PLLA-Ca means that about 20-26% of carboxyl ends are in calcium salt form.

Therefore, the end structures of PLLA-H would be mostly of the carboxylic acid and hydroxyl groups, while PLLA-Ca would mostly have the carboxylic acid and its calcium salt form, and hydroxyl group structures.

3.2. Pyrolysis products from PLLA-H and PLLA-Ca

Figure 1 shows the ^{1}H-NMR spectra of volatile degradation products from PLLA-H and PLLA-Ca that have undergone isothermal pyrolysis at 350ºC in a glass tube oven. In both spectra, lactides, as the major products, were found at 1.67 and 1.71 ppm for methyl protons of L,L-/D,D-lactides, and *meso*-lactide, respectively. For PLLA-H, some other peaks were detected at 1.4-1.6, 4.3-4.4, and 5.1-5.2 ppm. These peaks were assigned to methyl and methyne protons of cyclic and linear oligomers, using ^{1}H-^{1}H NMR (COSY) spectrum analysis. On the other hand, in the spectrum of PLLA-Ca, other products, except for lactides, were scarcely detected.

Figure 1. goes here

These volatile products were also analyzed by GC with a capillary column, cyclodextrin-β-236M-19, to split diastereoisomers. Figure 2 shows the GC chromatograph for

the volatile pyrolysis products of PLLA-H and PLLA-Ca. The peaks at 9.5, 12.5, and 13.1min were assigned to meso-, L, L-, and D, D-lactides by comparison with standard samples. It is obvious that, besides lactides, the pyrolysis products from PLLA-H contain many ingredients, whereas the products from PLLA-Ca contain only a few ingredients at 6.3 and 7.5 min, which were assigned to acetaldehyde and acrylic acid, respectively [15].

Figure 2. goes here

Figure 3. goes here

Table 1. goes here

In Figure 3, Py-GC-MS spectra of PLLA-H and PLLA-Ca pyrolysis products from 150~400°C are illustrated. A capillary column, Ultra Alloy^{+}-5, used in these measurements was suitable for analyzing these high boiling point products. Thus, cyclic oligomers were inspected in these spectra. A group of peaks, for example, Nos. 6-9, in which each peak showed an almost identical mass spectrum, was observed periodically. According to Kopinke et al. [15] and Khabbaz et al. [5], these groups represent the diastereoisomers of the cyclic oligomers. The peak assignment and relative content are listed in Table 1. It is obvious that lactides were the dominant pyrolysis products for both PLLA-H and PLLA-Ca. Quantitative analysis of the Py-GC-MS chromatogram showed that the lactides comprised about 67% of the PLLA-H pyrolysis products. On the other hand, a much higher figure of about 95% of PLLA-Ca degradation products were lactides..

3.3. Dynamic pyrolysis of PLLA–H and PLLA–Ca

To analyze differences in the thermal degradation behavior between PLLA-H and PLLA-Ca, the thermal degradation was studied by measuring the weight loss of the film samples as a function of linear increase in temperature in a nitrogen atmosphere using TG/DTA. Typical weight loss profiles for PLLA-H and PLLA-Ca at a heating rate (ϕ) 5°C min^{-1} are shown in Figure 4. The weight loss of PLLA-H started at about 280°C and then

smoothly decreased to reach almost complete degradation in a relatively narrow temperature range (280-370°C). On the other hand, the weight loss of PLLA-Ca began at a much lower temperature, about 220°C. The TG curve of PLLA-Ca extended over a rather wide range of temperature from 220 up to 360°C before complete decomposition. The molecular weight of PLLA-Ca (*Mn*=94,200, *Mw*=184,000) is lower than that of PLLA-H (*Mn*=138,000 *Mw*=253,000). Cam et al. reported that the decomposition temperature of PLLA rises with increase in the molecular weight. However, when *Mv* exceeds about 50,000, the decomposition temperature becomes almost constant [16]. Therefore, the difference in the pyrolysis temperature range between PLLA-H and PLLA-Ca could be ascribed to the difference of the end structure, but not to the molecular weight.

Figure 4. goes here

In differential thermogravimetric (DTG) curves of PLLA-H and PLLA-Ca samples (data not shown here), a gradual increase in weight loss was found at a lower temperature region. When the temperature rose to a higher point, each sample underwent a quick decomposition until weight loss was complete. This suggests that different plural decomposition pathways might be taken in the early and later periods of the PLLA pyrolysis. Kopinke et al. [13,15] have reported that for a PLLA containing Sn residue, at low temperature range, Sn-catalyzed depolymerization from free hydroxyl groups dominated. With the rising of temperature, several non-catalytic decomposition reactions randomly occurred inside the polymer chain. Aoyagi et al. [21] reported shoulders at a lower temperature region in DTG spectra in addition to a main peak at higher temperature region. They suggested that the shoulders might be attributable to aluminum-catalyzed depolymerization. However, our results suggest that, even if metal free, PLLA decomposition proceeds through plural pathways. Thus, the kinetics details are discussed in next section.

3.4. Kinetics studies on PLLA–H and PLLA–Ca

To clarify the decomposition pathways of PLLA-H and PLLA-Ca, a kinetics study on the pyrolysis was carried out. Some methods have already been established to evaluate the kinetic parameters from thermogravimetric data [26-34]. In this study the two well-known integral and differential methods and the improved random degradation analytical method [34], were employed to analyze the pyrolysis data of PLLA-H and PLLA-Ca.

Figure 5. goes here

Dynamic decomposition of both PLLA samples was carried out at different heating rates in TG/DTA. The thermograms at each heating rate ranging from 1~9 K min^{-1} for PLLA-H are illustrated in Figure 5, in which the TG traces have shifted to a higher temperature scale with increase in the heating rate. The temperature, T (K), for obtaining a certain fractional weight ratio value, w, at each heating rate should have the following relationship as a function of the heating rate ϕ [26].

$$\frac{d\log\phi}{d(1/T)} = -\frac{bEa}{R} \qquad (1)$$

where Ea and R are the apparent activation energy of the thermal degradation and the molar gas constant, respectively. And, b is a constant value in the Doyle's approximation Eq. (2) [27,28],

$$\log p(y) \cong -a - b\frac{Ea}{RT} \qquad (2)$$

in which $y = Ea/RT$ and a is a constant. When $y > 20$ in the function $p(y)$, then a and b are approximately 2.135 and 0.4567, respectively.

At a certain fractional weight ratio w, the apparent activation energy Ea was determined from the slope of the $\log(\phi)$ vs. $1/T$ plot. Figure 6 shows the $\log(\phi)$ vs. $1/T$ plot for PLLA-H at varied fractions from w=0.9 to 0.1. A straight line for each w was drawn by the least squares approximation method and Ea values at the varied fractions were calculated from the slopes

of these straight lines using the tentative *b* value, 0.4567. The results analyzed by this approach for PLLA-H and PLLA-Ca TG data are listed in Table 2.

Figure 6. goes here

Table 2. goes here

Using the obtained tentative *Ea* values, the function *y* values were calculated as about 32~46 and 18~25 in the temperature ranges of 250~390°C and 160~380°C for the pyrolysis of PLLA-H and PLLA-Ca, respectively. In these *y* value ranges, more accurate values of the constants *a* and *b* were recalculated as *a* = 2.3415, *b* = 0.4563 and *a* = 1.9205, *b* = 0.4703 for PLLA-H and PLLA-Ca, respectively. The apparent *Ea* values were re-determined using the recalculated *a* and *b* values (Table 2). For the PLLA-Ca sample, smaller *Ea* values were obtained at each fraction *w*.

Reich reported a method for estimating the *Ea* value at a specific fraction *w* from the TG data using the following Eq. (3) [30].

$$Ea = R\frac{\ln(T_1^2/\phi_1) - \ln(T_2^2/\phi_2)}{1/T_1 - 1/T_2} \qquad (3)$$

Based on Eq. (3), *Ea* values for both data of PLLA-H and PLLA-Ca pyrolysis were also calculated from the slopes of $\ln(T^2/\phi)$ vs. (1/*T*) plots. Results are listed in Table 2. From a comparison of the results in Table 2, the *Ea* values calculated by the corrected *a* and *b* values were used for the following analyses.

The *Ea* values for both PLLA-H and PLLA-Ca shifted to higher values as the fraction *w* decreased, indicating that the reaction mechanism changes with temperature and decomposition. However, a more detailed inspection of these *Ea* values reveals a difference in their tendency. It can be found that the *Ea* value of PLLA-H increased from about 140 to 176 kJ mol^{-1} at the first stage with a decrease in *w* from 0.9 to 0.5, and then kept constant at about 176 kJ mol^{-1} until almost complete decomposition had occurred. On the other hand, PLLA-Ca degraded at an almost constant value of 98 kJ mol^{-1} of *Ea* at the first stage with *w* in the range

of 0.9 to 0.5. The *Ea* value then gradually rose to about 120 kJ mol^{-1} in the following stage with a decrease in *w* from 0.5 to 0.1. These results are distinguishable from previous *Ea* values, 72-103 and 80-160 kJ mol^{-1} reported by Babanalbandi et al. [17] and Aoyagi et al. [21], in which metal contents were un-known.

If the pyrolysis of polymer proceeds through a fixed single pyrolysis process, the TG curves at different heating rates can be superposed upon each other by shifting them along the abscissa according to the following Eq. (4), which was derived from Eq. (1) [26].

$$\frac{1}{T_1} = \frac{1}{T_2} + \frac{R}{bEa}\left(\log\phi_2 - \log\phi_1\right) \tag{4}$$

Figure 7 shows the superpositions of thermograms of PLLA-H and PLLA-Ca pyrolysis as the plots of *w* vs. the right side in Eq. (4). A difference between the PLLA-H and PLLA-Ca superpositions can be clearly observed. For PLLA-H, when the *Ea* value 176 kJ mol^{-1} was used, the curves were scattered somewhat at the early stage of the pyrolysis, $w = 0.9\sim0.7$. At the later stage, there was convergence to a single curve. A reaction at the later stage would be a main degradation process of PLLA-H. Conversely, the superimposed curves of PLLA-Ca with the *Ea* value 98 kJ mol^{-1} show convergence in the first stage, $w > 0.5$. At a later stage, each curve was diverged. This implies that PLLA-Ca degraded by a way of a simple reaction at the first stage and, then, some other reactions occurred with the increase in weight loss.

Figure 7. goes here

The general integration equation for thermal degradation can be described asfollows:

$$-\int \frac{dw}{g(w)} = A\frac{Ea}{\phi R}\,p(y) = A\theta \tag{5}$$

in which $g(w)$ is a function whose form is related to the particular degradation reaction, but usually takes the form of w^n, where *n* is the order of reaction. Parameter *A* is the pre-exponential value and $\theta=(Ea/\phi R)p(y)$ is defined as the “reduced time” [26].

Ozawa [26] and Shimha et al. [31] reported the practical forms of $-\int dw/g(w)$ on some typical kinetic processes. For zero-, half-, 1st-, and 2nd-order reactions and random degradation

with the least unvolatilizable repeating units of 2 (L=2), $-\int dw/g(w)$ can be described as 1–w, 2(1-$w^{1/2}$), –ln$w$, (1-w)/w, and –ln{1-(1-w)$^{1/2}$}, respectively. Thus, comparing the experimental plot of w against $A\theta$ with the model ones should give more detailed kinetic information.

The PLLA-H data at a heating rate at 9 K min^{-1}, which can minimize the influence of minor reactions at a lower temperature range, were used for the kinetic analysis of PLLA-H pyrolysis to inspect the degradation path at the later main stage. The fraction w was plotted against $A\theta$ in Figure 8 with model reaction plots, in which Ea=176 kJ mol^{-1} was used. When A=2.0×10^{12} s^{-1} was used as the pre-exponential factor value, an acceptable agreement was obtained between the experimental data and the model simulations. At the early period, the experimental plot overlapped on the n^{th}-order model reaction plots. As w decreased, the experimental plot shifted on the random model reaction (L=4) plot. At the end of the pyrolysis, at which the temperature rose higher than 365ºC, the experimental data plot gradually deviated from the random model reaction (L=4) toward other random model reactions with higher L values. These results demonstrate that the PLLA-H degraded through the pathways of an n^{th}-order reaction at the first stage, and afterward followed a random reaction (L=4) as the main route.

Figure 8. goes here

A random degradation analysis was applied to determine the first stage reaction. For random degradations, a relationship between the fraction of broken bonds, α, and w can be described as [31],

$$w = (1-\alpha)^{L-1}\left\{1+\alpha\frac{(N-L)(L-1)}{N}\right\} \quad (6)$$

where α was described using the reduced time θ as: $\alpha = 1-e^{-A\theta}$. When $N >> L$, the following general expression is obtained [34],

$$\ln\left\{1-\left(1-\boldsymbol{w}\right)^{1/2}\right\}=-\frac{\boldsymbol{L}}{2}\boldsymbol{A}\theta+\ln\left\{\boldsymbol{e}^{\frac{\boldsymbol{L}}{2}\boldsymbol{A}\theta}-\left(\boldsymbol{e}^{\boldsymbol{L}\boldsymbol{A}\theta}-\boldsymbol{L}\boldsymbol{e}^{\boldsymbol{A}\theta}+\boldsymbol{L}-1\right)^{1/2}\right\} \quad (7)$$

When L = 2, this particular expression reduces to the following form [32,35],

$$\log[-\log\{1-(1-w)^{1/2}\}]=\log\frac{AEa}{2.3\phi R}-a-b\frac{Ea}{RT} \quad (8)$$

In Figure 9, plots of log[-log{1-(1-w)$^{1/2}$}] vs. 1/T for PLLA-H (9 K min^{-1}) and model reactions are shown. For each model random degradation expression, the left side of Eq. (7) exhibits nearly a linear relationship to 1/T. On the other hand, a characteristic curve is represented for each n^{th}-order model reaction. It was found that the experimental data plot obviously overlapped on the n^{th}-order reaction plots at the first stage, and shifted to a random reaction plot with L=4 in the following stage. At the end of the reaction, the data plots gradually shifted away from the random model reaction (L=4) plot, like the result obtained by the integration method.

Figure 9. goes here

Therefore, it is concluded that the pyrolysis of PLLA-H starts by an n^{th}-order reaction at the first stage and, then, shifts to a random degradation with L=4. The random degradation process can be regarded as the main process of PLLA-H pyrolysis. The apparent activation energy Ea and pre-exponential factor A values of this random degradation were evaluated to be 176 kJ mol^{-1} and 2.0×10^{12} s^{-1}, respectively.

In contrast to PLLA-H, the pyrolysis kinetics of PLLA-Ca was analyzed with the data at the lower heating rate, ϕ = 1 K min^{-1}, to clarify the reaction at the first stage. Figure 10 shows w vs. $A\theta$ plots of the experimental data and model reactions, in which Ea = 98 kJ mol^{-1} was used. When A = 8.4×10^5 s^{-1} was used as the pre-exponential factor, acceptable agreement was obtained between the experimental data and one of the model simulations. The experimental data plot was very close to the 1$^{\text{st}}$-order model reaction plot in the wide range of w > 0.2. This means that the PLLA-Ca degraded exclusively through the 1$^{\text{st}}$-order reaction process.

Afterwards, at the final stage of pyrolysis, the experimental data plot drifted away from the 1st-order reaction plot.

Figure 10. goes here

Figure 11. goes here

Analytical results of the PLLA-Ca data at ϕ = 1 K min^{-1} by the differential method is shown in Figure 11. The experimental $-dw/dT$ data were plotted against w with model reaction plots. Although scattering of the experimental data is marked, the experimental data plot approximated the 1st-order model reaction when Ea = 98 kJ mol^{-1} and $A = 8.4\times10^5$ s^{-1} were used as parameters. But at the initial period, the experimental data plot better approximated by the random model reaction rather than the 1st-order model reaction.

To determine the degradation behavior in the initial period, the random degradation analysis using the plot of $\log[-\log\{1-(1-w)^{1/2}\}]$ vs. $1/T$ was applied to the experimental data. The experimental data plot of PLLA-Ca (1 K min^{-1}) is shown in Figure 12 with model reaction plots, in which the same kinetic parameter values were employed. The main part of the experimental data plot agrees with the 1st-order reaction plot. However, at the initial period, the experimental data plot shifted from the 1st-order reaction plot, to become parallel to the random degradation simulations. Thus, a random degradation process is considered to occur at the initial period of the PLLA-Ca pyrolysis.

Figure 12. goes here

These results indicate that the main pyrolysis process of PLLA-Ca is a 1st-order degradation, but at the initial period the pyrolysis starts by a random degradation process. The kinetic parameters of this 1st-order reaction were estimated as the apparent activation energy Ea = 98 kJ mol^{-1} with a pre-exponential factor $A = 8.4\times10^5$ s^{-1}.

Therefore, the thermal degradation of PLLA-H and PLLA-Ca samples proceeds through peculiar kinetics routes with the different kinetic parameters. The estimated kinetic parameters, Ea, A, and the reaction order are summarized in Table 3.

Table 3. goes here

3.5. Mechanism of PLLA-H and PLLA-Ca pyrolysis

Generally, inter- and intra-molecular transesterification reactions are considered as the principal mechanism of PLLA pyrolysis [13]. Other reactions, such as *cis*-elimination and non-selective radical reactions, can also occur competitively [12-14]. From the kinetic studies, it was evaluated that the pyrolysis of PLLA-H proceeds mainly through the random degradation (L=4). The random degradation (L=4) means the distillation of cyclic and linear trimers and lower molecular weight products. The products of PLLA-H pyrolysis contained lactides, cyclic oligomers, and linear ingredients from the GC and ^{1}H-NMR analyses. Thus, the main mechanism of PLLA-H pyrolysis can be deduced as being the intra- and inter-molecular transesterification reactions, as shown in Scheme 1. However, the suggested n^{th}-order reaction at the first stage is not yet clear, though it may be caused by the residual Sn compounds.

Scheme 1. goes here

On the other hand, the thermal degradation of PLLA-Ca proceeds mainly through the 1^{st}-order reaction. The characterization of PLLA-Ca pyrolysis products revealed that the products are almost entirely composed of lactides. The 1^{st}-order reaction mechanism is considered to be the unzipping depolymerization, which would proceed through a back-biting attack by alkoxide end (Scheme 2). As mentioned in the foregoing section, the calcium ion in PLLA-Ca should be in the form of lactic acid salt and positioned at the carboxyl end. Therefore, at the start of the degradation, some kinds of transfer reactions (a) and (b) as shown in Scheme 3 might occur, in which the calcium ion moves to the alcohol end according to the reaction (b). These transfer reactions to ester groups are random degradation processes, but not a 1^{st}-order reaction. Therefore, the random reaction at the initial period of PLLA-Ca pyrolysis might be ascribed to these kinds of transfer reactions. But, the transfer reactions are

not determined clearly yet. This will be clarified by further investigation into the PLLA pyrolysis. The increase in *Ea* value in the later stage of PLLA-Ca decomposition is considered to be due to a pyrolysis of accumulated chain end residues, because it was not found in the PLLA-H pyrolysis, in which the random transesterification reactions would retard the accumulation of chain end residues.

Scheme 2. goes here

Scheme 3. goes here

4. Conclusions

The pyrolysis of PLLA was influenced by the different kinds of end structures, of the carboxyl and calcium ion end capped types. Thermogravimetric studies showed that the carboxyl-ended PLLA-H degraded in a relatively narrow temperature range of 280~370°C, whereas the calcium ion capped PLLA-Ca started to degrade at lower temperature, and this process extended over a wide temperature range of 220~360°C. From the kinetic analyses of TG data, the apparent activation energy, *Ea*, rose from 140 to 176 kJ mol^{-1} and from 98 to 120 kJ mol^{-1} with increase in weight loss and temperature for PLLA-H and PLLA-Ca pyrolysis, respectively. The kinetic studies also revealed that PLLA-H pyrolysis proceeds mainly through the random degradation (L=4), whereas PLLA-Ca decomposed through a 1^{st}-order reaction. For both samples, the dominant pyrolysis products were L,L-, D,D-, and *meso*-lactides. About 67% of the PLLA-H pyrolysis products were lactides, whereas the figure was about 95% for the PLLA-Ca pyrolysis products. Other oligomers were also detected in the Py-GC-MS chromatogram, especially for PLLA-H. Possible mechanisms for PLLA-H and PLLA-Ca pyrolysis were considered according to the random degradation (L=4) for PLLA-H and the unzipping depolymerization for PLLA-Ca. The results obtained in this study will provide instruction for the chemical recycling of poly(lactide).

Acknowledgments

This study was financially supported by Special Coordination Funds of the Ministry of Education, Culture, Sports, Science and Technology, the Japanese Government. The authors would like to thank Dr. Amin Cao, of the National Institute of Advanced Industrial Science and Technology (AIST), for the TG/DTA experiments.

References

[1] Ikada Y, Tsuji H. Biodegradable polyesters for medical and ecological applications. Macromol Rapid Commun 2000; 21(3): 117-32.

[2] Amass W, Amass A, Tighe B. A review of biodegradable polymers: Uses, current developments in the synthesis and characterization of biodegradable polyesters, blends of biodegradable polymers and recent advances in biodegradation studies. Polym Int 1998; 47(2): 89-144.

[3] Anderson JM, Shive MS. Biodegradation and biocompatibility of PLA and PLGA microspheres. Advan Drug Delivery Rev. 1997; 28 (1): 5-24

[4] Ajioka M, Enomoto K, Suzuki K, Yamaguchi A. The basic properties of poly (lactic acid) produced by the direct condensation polymerization of lactic acid. J Environm Polym Degrad 1995; 3(4): 225-34.

[5] Khabbaz F, Karlsson S, Albertsson AC. Py-GC/MS an effective technique to characterizing of degradation mechanism of poly (L-lactide) in the different environment. J Appl Polym Sci 2000; 78: 2369-78.

[6] Pranamuda H, Tokiwa Y, Tanaka H. Polylactide Degradation by an *Amycolatopsis* sp. Appl Environ Microbiol 1997; 63: 1637-40.

[7] Lunt J. Large-scale production, properties and commercial applications of polylactic acid polymers. Polym Degrad Stab 1998; 59: 145-52.

[8] Radano CP, Baker GL, Smith MR. Stereoselective polymerization of a racemic monomer with a racemic catalyst: direct preparation of the polylactic acid stereocomplex from racemic lactide. J Am Chem Soc 2000; 122: 1552-3.

[9] Kowalski A, Duda A, Penczek S. Mechanism of cyclic ester polymerization initiated with tin(II) octoate. 2. Macromolecules fitted with tin(II) alkoxide species observed directly in MALDI-TOF spectra. Macromolecules 2000; 33: 689-95.

[10] Kricheldorf HR, Kreiser-Saunders I, Stricker A. Polylactones 48. $SnOct_2$-initiated polymerization of lactide: a mechanistic study. Macromolecules 2000; 33: 702-9.

[11] Witzke DR, Narayan R. Reversible kinetics and thermodynamics of the homopolymerization of L-lactide with 2-ethylhexanoic acid tin(II) salt. Macromolecules 1997; 30: 7075-85.

[12] Leiper HA, McNeill IC. Degradation studies of some polyesters and polycarbonates-1. Polylactide: General features of the degradation under programmed heating conditions. Polym Degrad Stab 1985; 11: 267-85.

[13] Kopinke, FD, Mackenzie K. Mechanism aspects of the thermal degradation of poly(lactic acid) and poly (β-hydroxybutyric acid). J Anal Appl Pyrol 1997; 40-41: 43-53.

[14] Leiper HA, McNeill IC. Degradation studies of some polyeaters and polycarbonates-2. Polylactide: Degradation under isothermal conditions, thermal degradation mechanism and photolysis of the polymer. Polym Degrad Stab 1985; 11: 309-26.

[15] Kopinke FD, Remmler M, Mackenzie K, Moder M, Wachsen O. Thermal decomposition of biodegradable polysters-II. Poly (lactic acid). Polym Degrad Stab 1996; 53: 329-42.

[16] Cam D, Marucci M. Influence of residual monomers and metals on poly (L-lactide) thermal stability. Polymer 1997; 38: 1879-84.

[17] Babanalbandi A, Hill DJT, Hunter DS, Kettle L. Thermal stability of poly (lactic acid) before and after γ-radiolysis. Polym Int 1999; 48: 980-4.

[18] Lee SH, Kim SH, Han YK, Kim YH. Synthesis and degradation of end-group-functionalized polylactide. J Polym Sci Polym Chem Ed 2001; 39: 973-85.

[19] Zhang X, Wyss UP, Pichora D, Goosen MFA. An investigation of the synthesis and thermal stability of poly(DL-lactide). Polym Bull 1992; 27: 623-9.

[20] Jamshidi K, Hyon SH, Ikada Y. Thermal characterization of polylactides. Polymer 1988; 29: 2229-34.

[21] Aoyagi Y, Yamashita K, Doi Y. Thermal degradation of poly [(*R*)-3-hydroxybutyrate], poly [ε-caprolactone], and poly[(*S*)-lactide]. Polym Degrad Stab 2002; 76: 53-9.

[22] Schindler A, Harper D. Polylactide. II. Viscosity-molecular weight relationships and unperturbed chain dimensions. J Polym Sci Polym Chem Ed 1979; 17: 2593-99.

[23] Witzke DR, Narayan R, Kolstad JJ. Reversible kinetics and thermodynamics of the homopolymerization of L-lactide with 2-ethylhexanoic acid Tin(II) salt. Macromolecules 1997; 30: 7075-85.

[24] Nijenhuis AJ, Grijpma DW, Pennings AJ. Lewis acid catalyzed polymerization of L-lactide. Kinetics and mechanism of the bulk polymerization. Macromolecules 1992; 25: 6419-24.

[25] Kricheldorf HR, Saunders IK, Boettcher C. Polylactones: 31. Sn(II)octoate-initiated polymerization of L-lactide: a mechanistic study. Polymer 1995; 36: 1253-9.

[26] Ozawa T. A new method of analyzing thermogravimetric data. Bull Chem Soc Japan 1965; 38:1881-6.

[27] Doyle CD. Kinetics analysis of thermogravimetric data. J Appl Polym Sci 1961; 5: 285-92.

[28] Doyle CD. Estimating isothermal life from thermogravimetric data. J Appl Polym Sci 1962; 6: 639-42.

[29] Flynn JH, Wall LA. A quick, direct method for the determination of activation energy from thermogravimetric data. Polym Lett 1966; 4: 323-8.

[30] Reich L. A rapid estimation of activation energy from thermogravimetric traces. Polym Lett 1964; 2: 621-3.

[31] Simha R, Wall LA. Kinetics of chain depolymerization. J Phys Chem 1952; 56: 707-15.

[32] Flynn JH, Wall LA. General treatment of the thermogravimetry of polymers. J Res Nat Bur Stand 1966; 70A: 487-523.

[33] Ichihara S, Nakagawa H, Tsukazawa Y. Thermal decomposition behaviors of polymers analyzed with thermogravimetry. Kobunshi Ronbunshu 1994; 51(7): 459-65.

[34] Nishida H, Yamashita M, Endo T. Analysis of initial process in pyrolysis of poly (*p*-dioxanone). Polym Degrad Stab 2002; 78: 129-135.

[35] Okamura S, Yamaoka H, Tsuji K. editors. Polymer no Bunkai. Kyoto: Kagaku Dojin, 1974. p. 195.

Figure and Scheme Captions

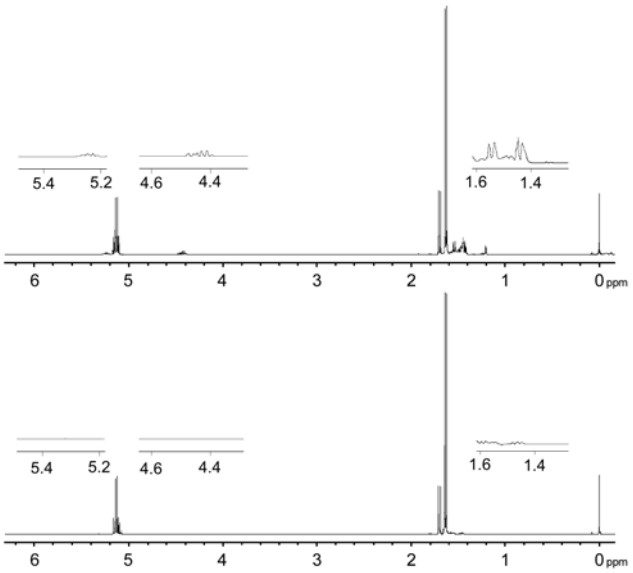

Figure 1. ^{1}H-NMR spectra of volatile degradation products from PLLA-H (upper) and PLLA-Ca (lower) on isothermal pyrolysis at 350°C in a glass tube oven.

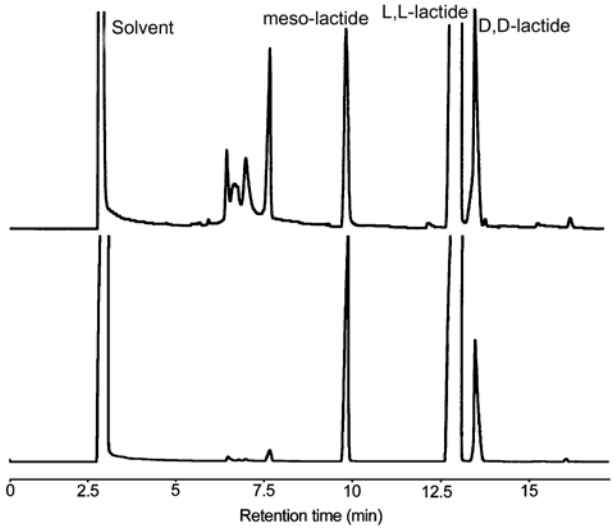

Figure 2. GC chromatograms for volatile pyrolysis products of PLLA-H (upper) and PLLA-Ca (lower).

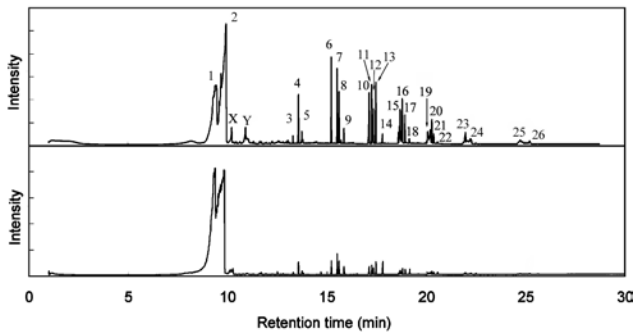

Figure 3. Py-GC-MS total ion current spectra of PLLA-H (upper) and PLLA-Ca (lower) pyrolysis products from 150-400°C.

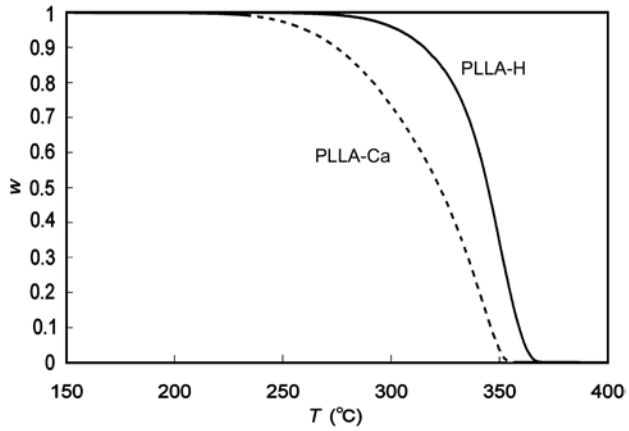

Figure 4. Thermogravimetric curves of PLLA-H and PLLA-Ca decomposition at a heating rate of 5 K min^{-1} under N_2 flow of 100 mL min^{-1}. PLLA-H, solid line; PLLA-Ca, broken line.

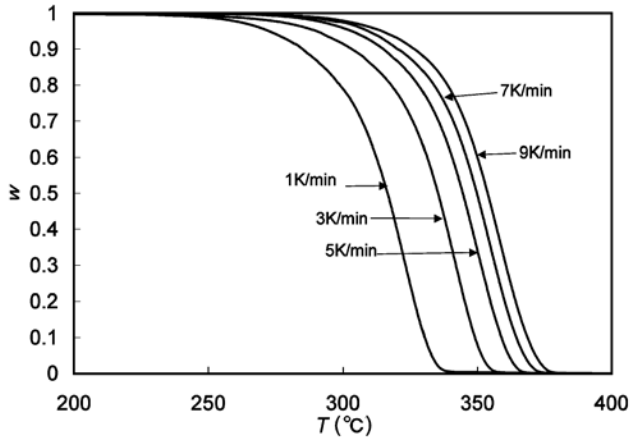

Figure 5. Thermogravimetric curves of PLLA-H decomposition at heating rates of 1, 3, 5, 7, and 9 K min^{-1} under N_2 flow of 100 mL min^{-1}.

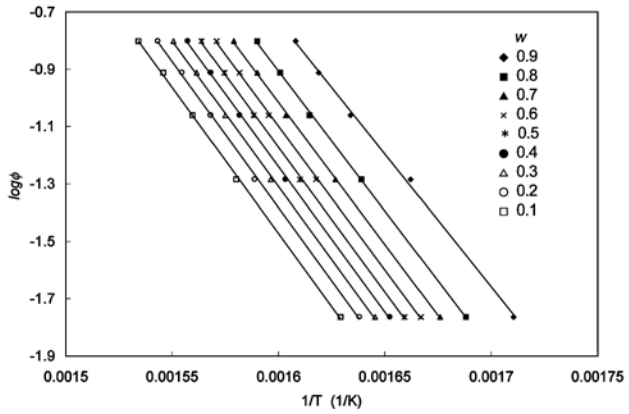

Figure 6. Plots of logϕ vs. 1/T at varied fractions from w = 0.9 to 0.1 for PLLA-H decomposition.

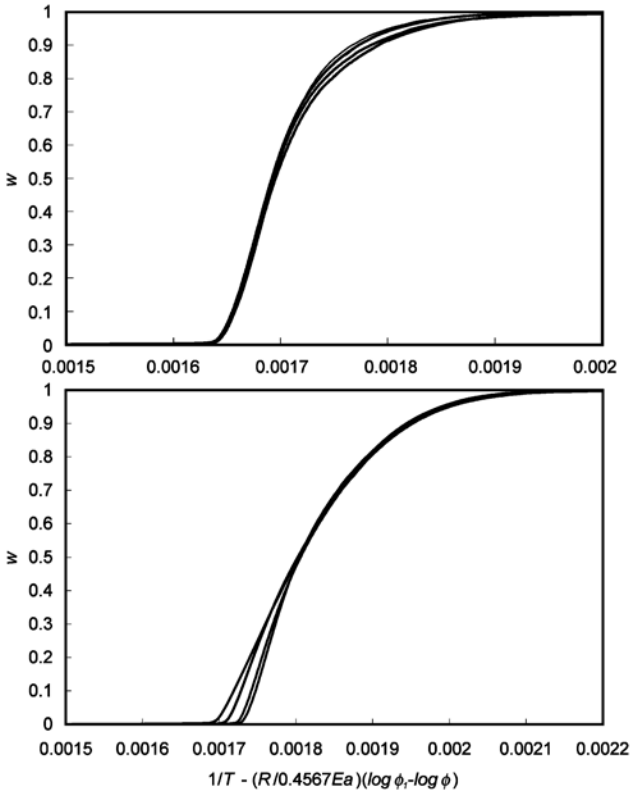

Figure 7. Superpositions of thermogravimetric curves of PLLA-H (upper, Ea=176 kJ mol^{-1}) and PLLA-Ca (lower, Ea=98 kJ mol^{-1}) decomposition at heating rates of 1, 3, 5, 7, and 9 K min^{-1}.

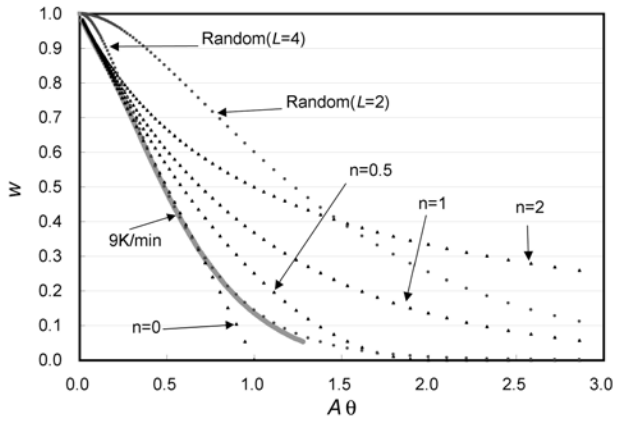

Figure 8. Plots of experimental $(AEa/\phi R)p(y)$ $(=A\theta)$ vs. w of PLLA-H at a heating rate 9 K min^{-1} (Ea=176 kJ mol^{-1}, A=2.0×10^{12} s^{-1}), and $-\int dw/g(w)$ vs. w for model reactions. Model reactions: zero (n=0), half (n=0.5), 1st (n=1), and 2nd-order (n=2), and random degradations (Random L=2 and 4).

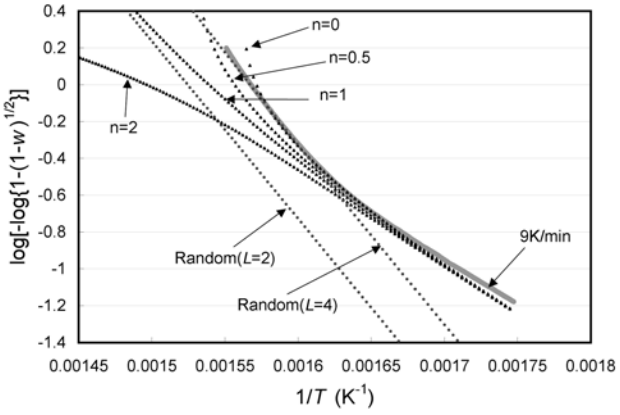

Figure 9. Plots of log[-log{1-(1-w)$^{1/2}$}] vs. 1/T for thermogravimetric data of PLLA-H at a heating rate of 9 K min^{-1} (Ea=176 kJ mol^{-1}, A=2.0×10^{12} s^{-1}), and for model reactions Model reactions: zero (n=0), half (n=0.5), 1st (n=1), and 2nd-order (n=2), and random degradations (Random L=2 and 4).

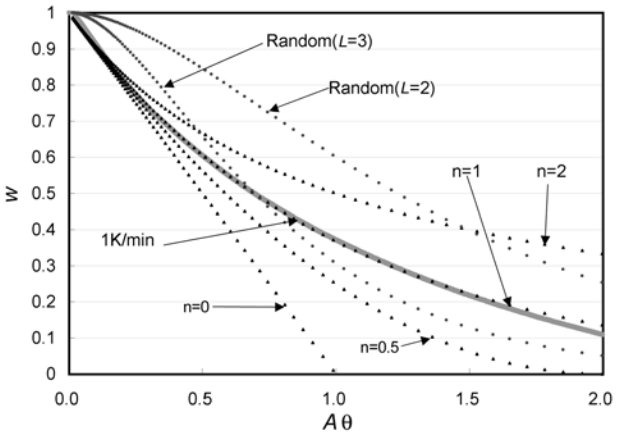

Figure 10. Plots of experimental ($AEa/\phi R$)$p(y)$ ($=A\theta$) vs. w of PLLA-Ca at a heating rate 1 K min^{-1} (Ea=98 kJ mol^{-1}, A=8.4×10^5 s^{-1}), and $-\int dw/g(w)$ vs. w for model reactions. Model reactions: zero (n=0), half (n=0.5), 1st (n=1), and 2nd-order (n=2), and random degradations (Random L=2 and 3).

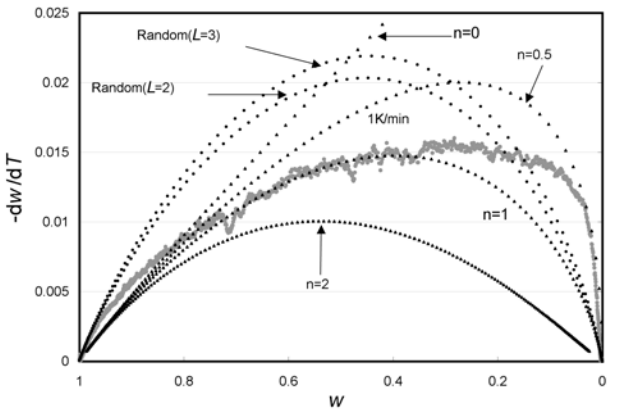

Figure 11. Plots of experimental $-dw/dT$ vs. w of PLLA-Ca at a heating rate 1 K min^{-1} (Ea=98 kJ mol^{-1}, A=8.4×10^5 s^{-1}), and (A/ϕ)exp(-Ea/RT)g(w) vs. w for model reactions. Model reactions: zero (n=0), half (n=0.5), 1st (n=1), and 2nd-order (n=2), and random degradations (Random L=2 and 3).

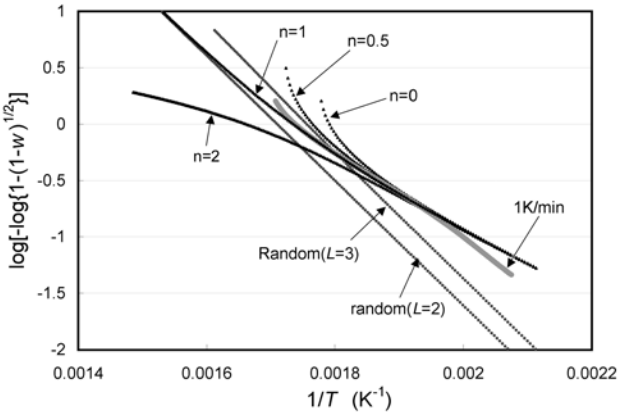

Figure 12. Plots of log[-log{1-(1-w)$^{1/2}$}] vs. 1/T for thermogravimetric data of PLLA-Ca at a heating rate of 1 K min^{-1} (Ea=98 kJ mol^{-1}, A=8.4×10^5 s^{-1}), and for model reactions. Model reactions: zero (n=0), half (n=0.5), 1st (n=1), and 2nd-order (n=2), and random degradations (Random L=2 and 3).

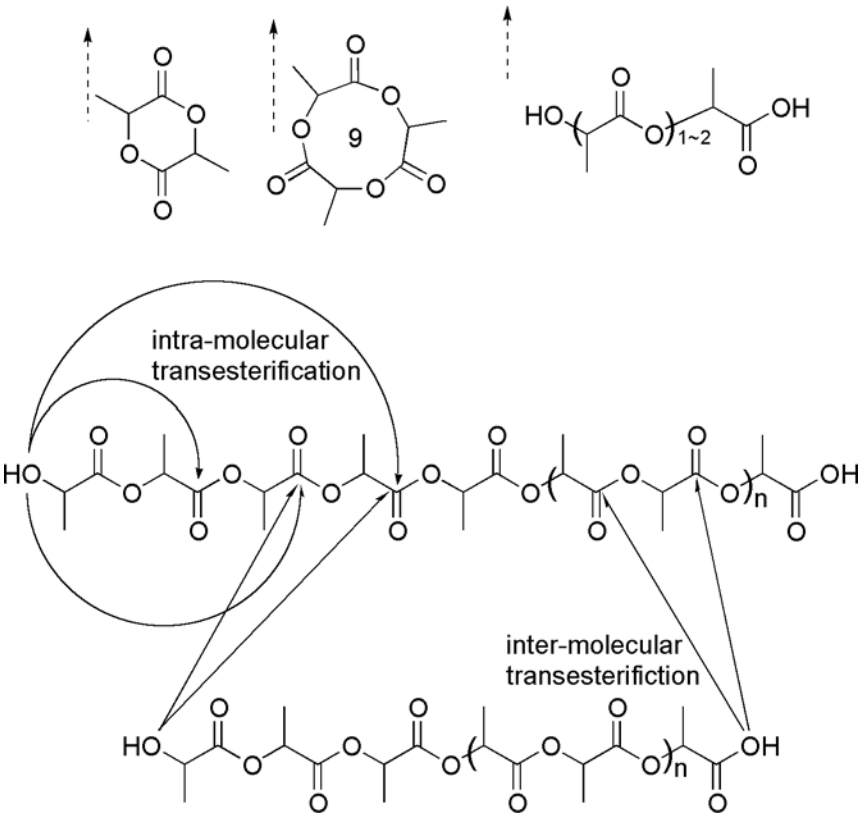

Scheme 1. Main transesterification reactions of PLLA-H decomposition.

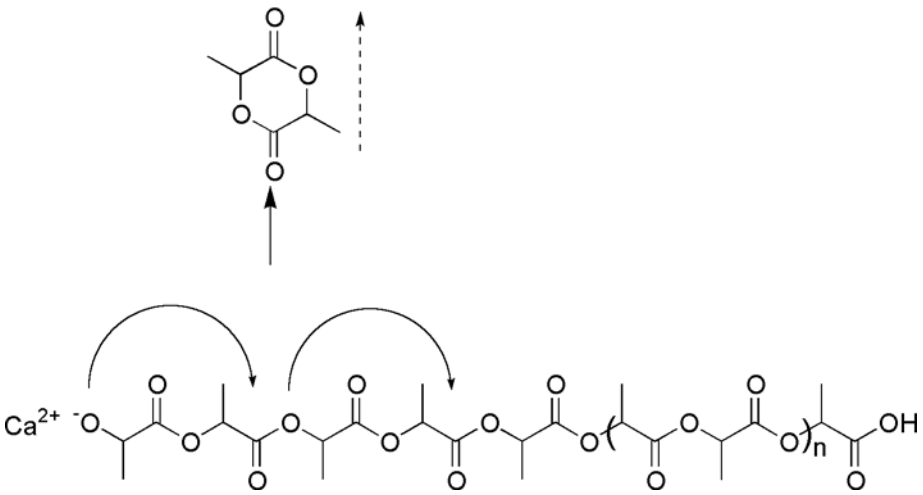

Scheme 2. Main unzipping depolymerization of PLLA-Ca decomposition.

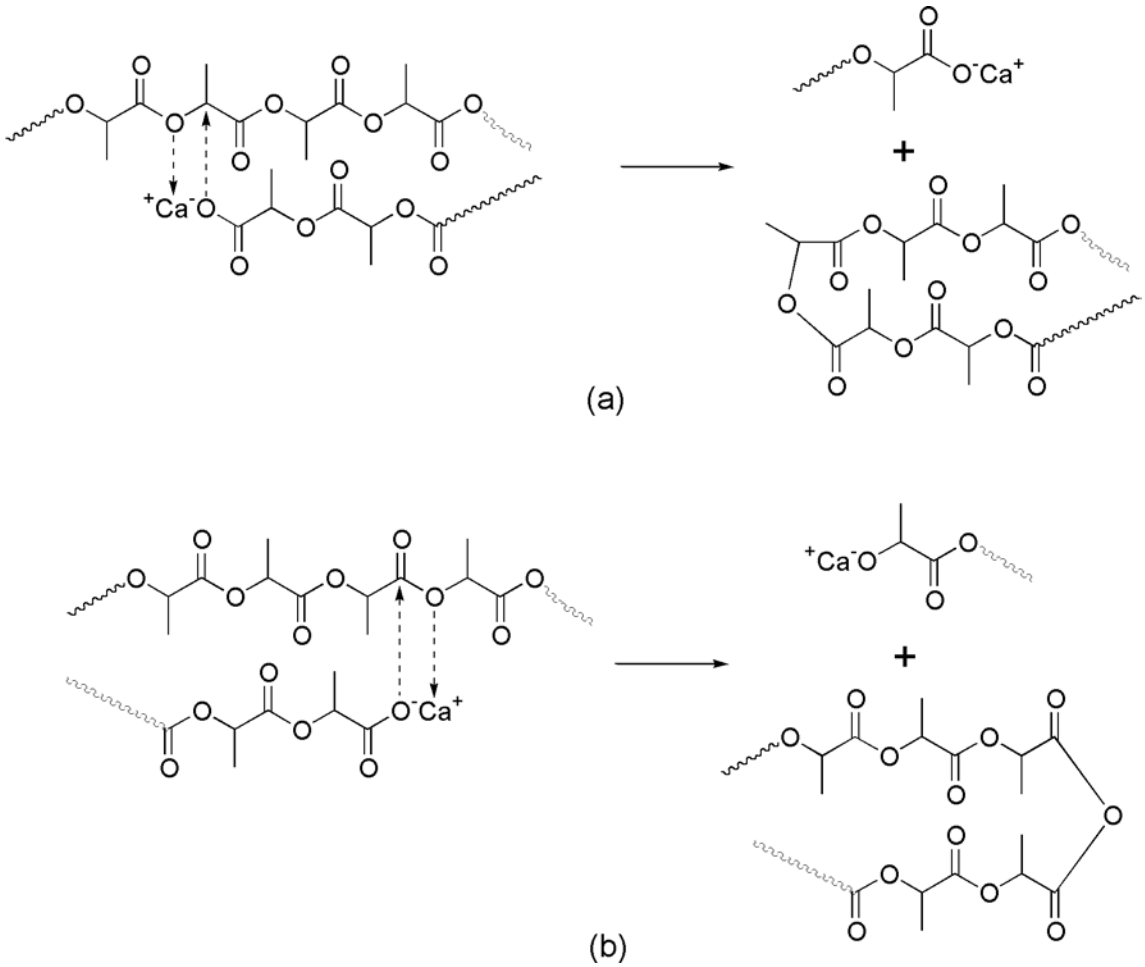

Scheme 3. Possible random transfer reactions at the start of PLLA-Ca decomposition.

Table 1. Relative content of pyrolysis products in the Py-GC-MS chromatograms for PLLA-H and PLLA-Ca decomposition

Peak No.	Products	Relative content (%)	
		PLLA-H	PLLA-Ca
1	*meso*-lactide	24.0	35.8
2	D, L-lactide	43.8	59.0
3-5	Trimer	2.3	0.6
6-9	Tetramer	7.2	0.5
10-14	Pentamer	8.1	1.8
15-18	Hexamer	6.2	0.7
19-22	Heptamer	3.7	0.5
23, 24	Octamer	0.9	–
25, 26	Nonamer	1.2	–
X	Unidentified	1.0	1.1
Y	Unidentified	1.6	–

Table 2. Activation energy, *Ea*, of PLLA-H and PLLA-Ca pyrolysis

w	PLLA-H			PLLA-Ca		
	Eq. (1)		Eq. (3)	Eq. (1)		Eq. (3)
	Ea (kJ mol^{-1})		*Ea* (kJ mol^{-1})	*Ea* (kJ mol^{-1})		*Ea* (kJ mol^{-1})
	a=2.315 b=0.4567	a=2.2921 b=0.4576		a=2.315 b=0.4567	a=1.9622 b=0.4686	
0.9	141.3	141.4	139.0	103.9	100.9	100.4
0.8	153.5	153.6	151.6	101.0	98.1	97.1
0.7	164.4	164.6	162.9	100.9	98.0	96.8
0.6	169.7	169.8	168.4	100.6	97.7	96.3
0.5	173.6	173.7	172.4	102.0	99.0	97.6
0.4	175.3	175.4	174.2	105.4	102.4	101.2
0.3	176.5	176.6	175.4	110.4	107.2	106.3
0.2	176.9	177.1	175.8	116.2	112.9	112.3
0.1	176.3	176.4	175.0	124.0	120.4	120.4
Mean	167.5	167.6	166.1	107.2	104.1	103.1

Table 3. Kinetic parameters for PLLA-H and PLLA-Ca pyrolysis

Sample	*Ea* (kJ mol^{-1})	*A* (s^{-1})	*n* / *random*	*Ea* (kJ mol^{-1})	*A* (s^{-1})	*n* / *random*
PLLA-H	First stage (w = 0.9)			Main stage (w = 0.5~0.1)		
	140		n^{th}	176	2.00×10^{12}	random(L=4)
PLLA-Ca	Initial period			Main stage (w=1~0.4)		
			random	98	8.40×10^{5}	1^{st}